doi:10.3788/gzxb20174606.0614001

大功率 1 060 nm 双沟脊波导分布反馈激光器

王薇，翟腾，王皓，谭少阳，王圩，张瑞康，吉晨
（中国科学院半导体研究所 材料重点实验室，北京 100083）

摘 要：研制了双沟型脊波导结构的 1 060 nm 分布反馈激光器.和普通脊波导激光器相比，该器件能提高在连续条件下的侧模稳定性.单模最大输出功率达到 300 mW 边模抑制比大于 45 dB.采用该激光器进行泵浦周期性极化铌酸锂晶体倍频实验，得到的绿光功率为 3 mW，该方案将成为低成本绿光光源实现方案.

关键词：大功率；分布反馈激光器；双沟脊波导；单模；二次谐波
中图分类号：O439 **文献标识码**：A **文章编号**：1004-4213(2017)06-0614001-6

High Power 1 060 nm Distributed Feedback Semiconductor Laser with Double-Trench Ridge Waveguide Structure

WANG Wei, ZHAI Teng, WANG Hao, TAN Shao-yang, WANG Wei, ZHANG Rui-kang, JI Chen
(*Key Laboratory of Semiconductors Materials, Institute of Semiconductors, Chinese Academy of Sciences, Beijing* 100083 *China*)

Abstract: In this letter a 1 060 mm distributed feedback laser with an optimized double-trench ridge waveguide structure is presented. The lateral mode stability is strongly improved under continuous-wave operating condition. The maximum single spectral and spatial mode output power is approximately 300 mW with a side mode suppression ratio larger than 45 dB. The capability of the device for green light generation is also demonstrated experimentally by pumping a periodically poled lithium niobate waveguide crystal, which the power of the green light is about 3 mW.

Key words: High power; Distributed feedback; Double-trench ridge waveguide; Single-mode; Second harmonic generation
OCIS Codes: 140.5960; 140.3570; 140.3490; 140.3515

0 Introduction

High-power single-mode semiconductor laser diodes emitting at wavelength near 1 μm have many important applications in many fields such as communication, spectroscopy and frequency conversion[1,2]. It is possible to replace solid and fiber lasers for their advantages of high efficiency, low cost, high reliability and compact size. Particularly in laser display system semiconductor laser diodes emitting at wavelength of 1064 mm of great importance to generate green light by means of Second Harmonic Generation (SHG)[3-5]. The light source suitable for the SHG should have a narrow spectral linewidth below the acceptance bandwidth of the MgO-doped Periodically Poled Lithium Niobate (PPLN) waveguide crystal for the SHG (typically smaller than 200 pm). Distributed Bragg Reflector (DBR) lasers[6] or Distributed Feedback (DFB) lasers[4] can be applied to obtain single wavelength emission. However, DBR lasers suffer from periodic nonlinearities in the light-current characteristics and longitudinal mode hopping

Foundation item: The National Natural Science Foundation of China (Nos. 61274046, 61474111, 61271066)
First author: WANG Wei (1991—), female, M. S. degree, mainly focused on high power semiconductor lasers. Email:weiwang14@semi.ac.cn
Contact author: ZHANG Rui-kang (1973—), male, senior engneer, mainly focuses on semiconductor laser research. Email: rkzhang@semi.ac.cn
Received: Dec. 30, 2016; **Accepted**: Mar. 13, 2017

between adjacent Fabry-Perot(FP) modes[7]. In contrast, DFB lasers inherently, can operate in single mode over a large current range. Although DFB lasers emitting with wavelength of 1.3 and 1.55 μm have been widely developed for optical communication system, the study of single mode DFB lasers emitting at 1060 mm with hundreds of milliwatts is still limited.

To reach a higher single-mode output power, high current injection is essential for semiconductor lasers, which results in lateral refractive index variations. The variations usually bring higher order lateral modes and degrades the spectrum quality and beam quality of the lasers. High power DFB lasers demand that careful attention be paid to the design of the waveguide structure to suppress higher order lateral mode lasing. Currently various techniques have been developed. For example, extra loss discrimination is induced for higher order modes by forming an implanted absorption region[8-9] along the waveguide, or bending the waveguide[10]. However these approaches increase the loss of fundamental mode as well and the procedures are complex. Another approach to increase loss of the higher order mode is achieved by forming a double-trench ridge waveguide[11] which induces leaky loss for higher order lateral mode. By properly selecting the trench parameters, such as trench width, and trench depth, the leakage loss of fundamental mode can be negligible, while that of higher order mode is high enough to suppress the modes lasing.

In semiconductor laser long cavity length design is essential for high power operation, which requires low internal loss of the cavity to ensure the high efficiency of the device. The device internal loss is mainly attributed to free carrier absorption in p- and n-cladding layers[12]. So the waveguide structure should be optimized to minimize the internal loss as well.

Previously 1064 mm DFB lasers with a single-mode output power of 150 mW[13] and 90 mW have been reported by our group. In those lasers high order lateral modes begin to lase at high injection level and limit them to reach higher single-mode output powers. In this letter we present an optimized 1 060 mm DFB laser with a double-trench ridge waveguide design. The single lateral mode stability is strongly improved and the maximum single mode output power is approximately 300 mW with a SMSR larger than 45 dB. The capability of the device for green light generation is also demonstrated experimentally by pumping a PPLN crystal.

1 Design and fabrication

In order to reduce the internal loss, the material composition and thickness should be optimized for each epitaxial layers. Fig. 1 shows an energy band diagram of a 1 060 nm laser structure developed by our group, the laser included the $Al_{0.47}Ga_{0.53}As$ cladding layer, the InGaAs/GaAs Double Quantum-Wells (DQW) embedded in the GaAs waveguide layer and the $Al_{0.26}Ga_{0.74}As$ step cladding layer, and GaAs contact layers. The value of W refers to the GaAs Separate Confinement Heterostructure (SCH) waveguide width. In our work Broad Area (BA) lasers with four different W of 15, 50, 200, and 400 mm are grown by metalorganic chemical vapor deposition (MOCVD) and fabricated by standard processes. The internal loss of the laser has been determined experimentally and the value of W are optimized combined with simulation results.

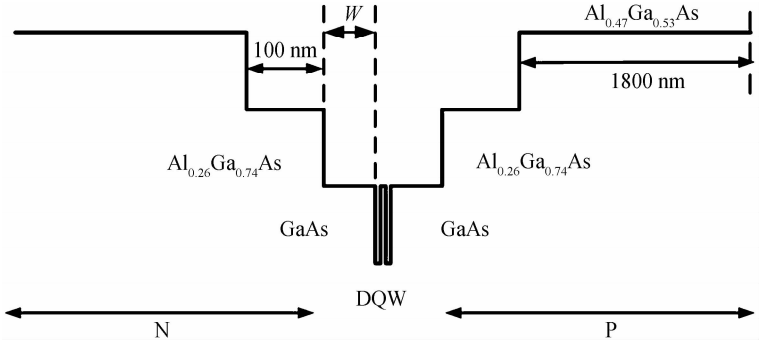

Fig. 1 Energy band diagram of the SCH waveguide laser

On this basis the 1 060 nm DFB laser is designed and fabricated. The vertical structure of the laser is identical with BA laser structure except a 140 mm GaAs/InGaP grating layer is inserted under p-cladding

layer as shown in Fig. 2. After first MOCVD growth, a second-order grating with a period around 315 mm is formed on the grating layer by holographic photolithography and chemical etching. The duty cycle of the second order grating is optimized around 0.75 to obtain feedback from the second order grating. The photoresist is removed and surface cleaning is conducted after the grating fabrication. In the second growth step, following a 50 mm GaAs, the p-$Al_{0.47}Ga_{0.53}As$ cladding layer and the heavily p-doped GaAs contact layer are grown. Fig. 3 shows the Scanning Electron Microscope (SEM) image of the Bragg grating after overgrown. The coupling efficiency of the grating is estimated to be 20 cm^{-1} based on coupled mode analysis.

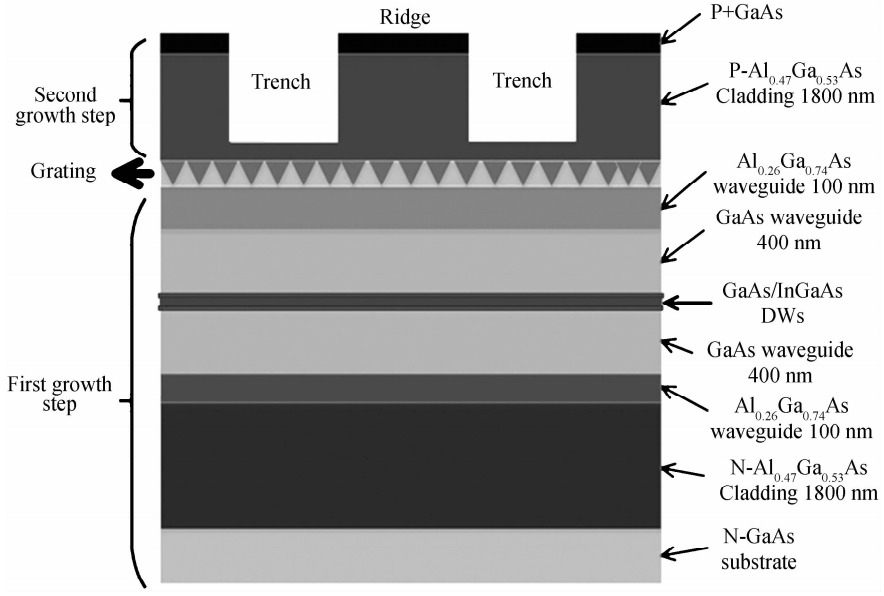

Fig. 2 Schematic diagram of the ridge waveguide DFB lasers

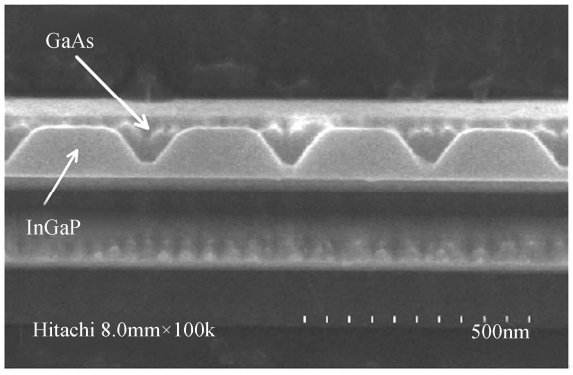

Fig. 3 SEM image of the cross section of the overgrown grating

The post growth procedure is as follow, lateral optical confinement is provided by a 3 μm wide strip. Double-trench leaky waveguide as shown in Fig. 2 is adopted to suppress higher order lateral modes. Inductively Coupled Plasma (ICP) etching is employed to get a lower vertical loss waveguide. The etching rate is controlled to be about 500 mm/min. A laser interferometer is used to monitor the etching process and etching depth in real time. The etching is stop at the center of the $Al_{0.26}Ga_{0.74}As$ step cladding layer. This depth leads to an effective refractive index difference (Δn_{eff}) between the region underneath the ridge and the region outside the ridge is about 0.003. The trench width is 4.5 μm which is optimized to induce leaky losses for higher lateral order modes with negligible effect to fundamental mode. Carrier confinement is realized with a SiO_2 insulation layer which is opened on top of the ridge waveguide. In the next step vacuum deposition of Ti/Au is performed. Finally, the wafer is lapped to 100 μm to make chip cleaving possible, and backside ohmic contact is made by AuGeNi/Au metallization after backside polishing. After the process, the wafer is cleaved into laser bars with device length of 2 mm. Front and back facets are coated with reflectivities of 0.1% and 95%, respectively in order to enhance the power output. Finally the

bars are cleaved into single laser chips and mounted p-side up onto heat sinks and characterized at 25℃.

2 Device testing and discussion

2.1 BA laser testing and discussion

The device internal loss is mainly attributed to free carrier absorption in p- and n-cladding layers. The internal loss of the laser has been determined experimentally by measuring the external quantum efficiencies and plotting their reciprocal value as the function of cavity length. As a example Fig. 4 shows the experimental result of the broad area laser with W of 50 nm. The internal parameters of $\eta_i=0.62$, $\alpha_i=3\ \mathrm{cm}^{-1}$ is extracted. For a Separate Confinement Heterostructure (SCH) quantum well semiconductor laser, as is shown in Fig. 1, the internal loss can be calculated by [12]

$$\alpha_i=\Gamma_{QW}\alpha_{QW}+\frac{1}{P}\int_{NCL}\sigma_n n(x)\,|E(x)|^2\mathrm{d}x+\frac{1}{P}\int_{PCL}\sigma_p p(x)\,|E(x)|^2\mathrm{d}x$$

where Γ_{QW} is the optical confinement factor of QW layers, α_{QW} is the material loss of quantum well from free carrier absorption; $n(x)$, $p(x)$ are the electrons and holes distribution of n- and p-doped cladding layers, respectively. $E(x)$ is the one dimensional electric-field distribution of fundamental TE modes in the transversal waveguide, and σ_n, σ_p are the absorption cross sections of the electrons and holes, respectively, which are determined experimentally[14]. Carrier density and eletric-field distribution were calculated by commercial software (Crosslight). According to the relationship above, the internal loss can be calculated. In our calculation $\delta_n=6\times10^{-18}\,\mathrm{cm}^{-2}$ and $\delta_p=14\times10^{-18}\,\mathrm{cm}^{-2}$ are used[14] and the doping level of n- and p-cladding layers are around $1\times10^{18}\,\mathrm{cm}^{-3}$ and $2\times10^{18}\,\mathrm{cm}^{-3}$, repensitively. Fig. 5 shows the simulated internal losses of BA lasers with different W value. With increasing the W value, the internal loss of the device is decreases as shown in Fig. 5, which is attributed to the decreasement of the overlap of p- and n-cladding layer and optical field. The experimentally determined are also shown in Fig. 5, which is consistent with simulated results. The internal loss of the device is less than 0.97 cm^{-1} when W is 400 mm. The change of internal loss level off for further increasing the W value and too thick waveguide layer will support multiple transverse modes, so we choose 400 mm as the optimum value for DFB laser design.

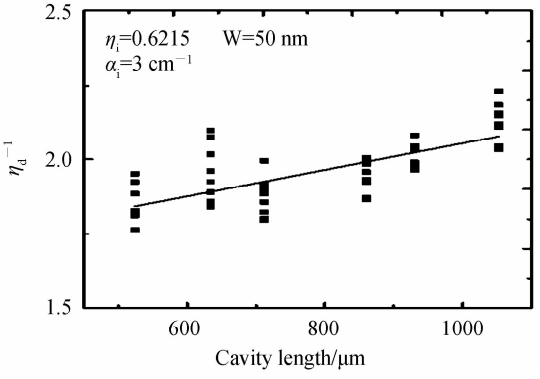

Fig. 4 Inverse external differential quantum for BA lasers with different width of GaAs waveguide

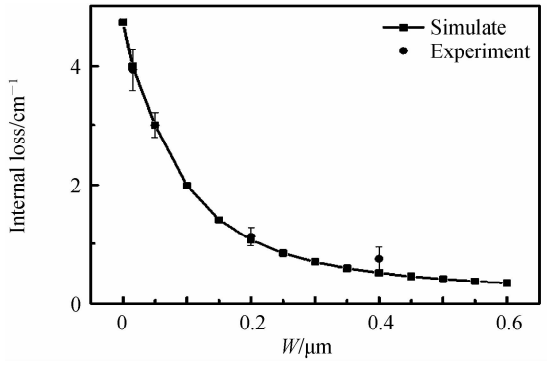

Fig. 5 Simulated and experimentally determined internal lossefficiency $1/\eta_d$ as a function of cavity length

2.2 DFB laser testing and discussion

Fig. 6 shows the Power-Current (PI) characteristics of the DFB laser under continuous-wave operating condition. The threshold current of the DFB laser is about 70 mA and the slope efficiency is about 0.52 W/A at the vicinity of threshold condition. The relatively large threshold current may be attributed to the defects induced by ICP etch process and can be improved by optimizing the ICP etch process. The device is operated in FP mode at low current injection level because of an excessive negative-offset between the gain spectrum of InGaAs/GaAs quantum wells and the Bragg wavelength. With current increasing, the gain spectrum is red shifted which is attributed to the joule heat. The negative-offset is decreased and the laser begin to operate in single mode when injection current above 220 mA. The laser maintains single mode and the kink-free power is up to approximately 300 mW. Comparing to our previous results[12-13], the strongly improvement of single-mode outpower is attributed to the optimized double-trench ridge waveguide design. An optical spectrum measured at 800 mA is shown in the inset of Fig. 5. The peak

wavelength is 1062.8 mm and the Side Mode Suppression Ratio (SMSR) is larger than 45 dB. Spectrum measurement confirmed the kink near 220 mA is attributed to the transition from FP mode to DFB mode.

The measured lateral and vertical far-fields intensities of the DFB-laser are summarized in Fig. 7. The parallel and vertical far-field has a Full Width at Half-Maximum angle (FWHM) of $\theta_{//}=8°$ and $\theta_{\perp}=47°$. The far-field profiles are Gaussian-shape peaks for all currents up to 800 mA, which confirms the laser preform a stable fundamental mode.

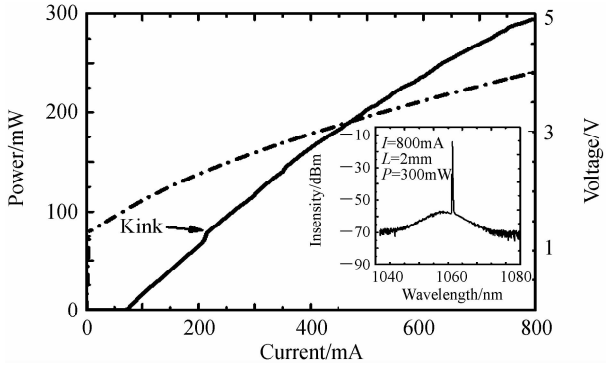

Fig. 6 Typical power-current characteristics of the DFB laser. The insert is the optical spectrum at biased current of 800 mA

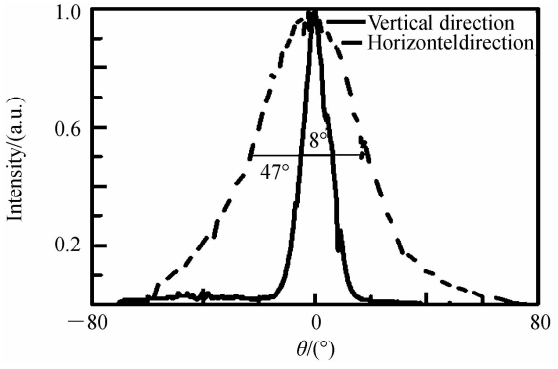

Fig. 7 Far-field profile of the DFB laser under CW condition at 25 ℃. (I=800 mA)

2.3 Second-harmonic generation

This DFB laser is ideally suitable for SHG due to the narrow spectral linewidth and high output power. Fig. 7 shows the optical path diagram for SHG experiment. In this paper, the nonlinear crystal used in the experiment is 5% MgO-doped PLLN waveguide crystals mainly in order to prevent photorefractive damage of the crystal. The first-order quasi-phase matching polarization period is 6.9 μm, with the duty ratio 1∶1. And the crystal length is 7 mm, the conversion efficiency is typical of 600% ~ 700%/W·cm^2. The light emitted from the DFB laser with the current of 800 mA is launched to a PPLN waveguide crystal through a wedge shaped polarization-maintaining optical fiber (PMF). Polarization controller is used to control the polarization direction of the pumping light in order to maximize the SHG efficiency. The spectral acceptance of the SHG waveguide crystal shifts with about 0.108 mm/K and allows to match to the spectral position of DFB laser with the help of the thermoelectric cooler (TEC). Eventually we got the green light from output fiber as shown in Fig. 8. The power of green light is about 3 mW. The relatively low convention efficiency is attributed to the low couple efficiency of DFB laser to

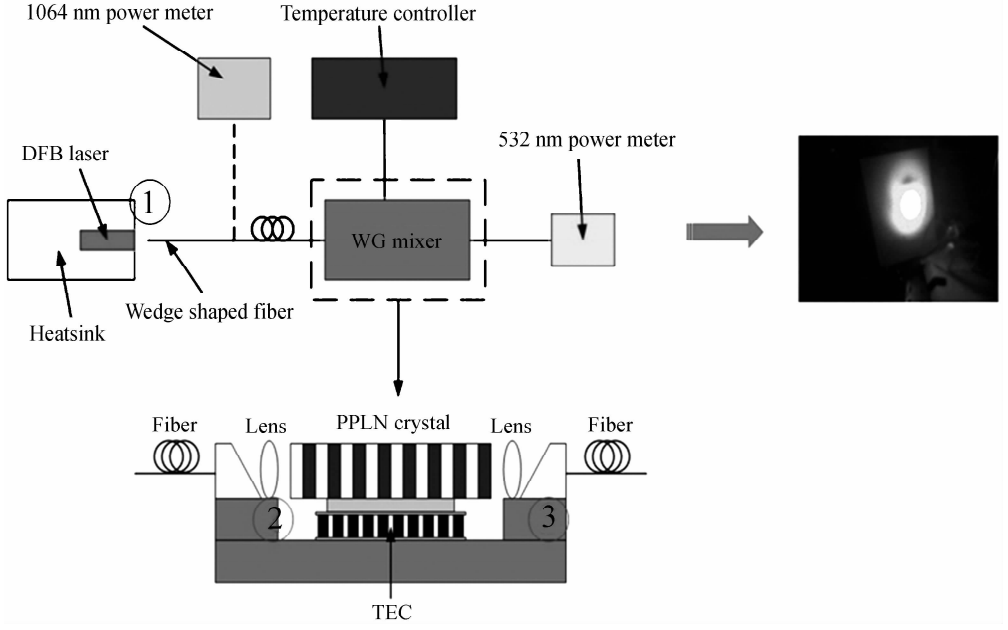

Fig. 8 Schematic diagram of SHG experiment. The picture on the right side of the arrow shows the generated green-light

PMF, which is about 20% only. Further optimizations of the laser will be concentrated on increasing the fiber couple efficiency of the laser.

3 Conclusion

In summary, we have demonstrated a 1 060 mm DFB laser. By systematically optimizing laser structure, single lateral mode stability is improved by employing a double-trench ridge waveguide design. A single-mode output power of 300 mW with a SMSR larger than 45 dB is obtained. Green light generated by pumping a PPLN waveguide crystal with the DFB laser has also been reported.

References

[1] DONG Zhen, ZHAO Yi-hao, ZHANG Qi, *et al*. High power 980 nm broad area distributed feedback laser with first-order gratings[J]. *Journal of Semiconductors*, 2016,**37**(2):024010.

[2] GONG Xue-qin, FENG Shi-wei, YUE Yuan, *et al*. Thermal analysis in high power GaAs-based laser diodes[J]. *Journal of Semiconductors*, 2016,**37**(4):044011.

[3] NGUYEN H K, COLEMAN S, VISOVSKY NJ, *et al*. Reliable high-power 1060 nm DBR lasers for second-harmonic generation[J]. *Electronics Letters*,2007,**43**(13):716-717.

[4] HONG K N, HU M H, NISHIYAMA N, *et al*. 107-mW low-noise green-light emission by frequency doubling of a reliable 1060-nm DFB semiconductor laser diode[J]. *IEEE Photonics Technology Letters*,2006,**18**(5):682-684.

[5] DEKKER P, BURNS P A, DAWEs J M, *et al*. Widely tunable yellow-green lasers based on the self-frequency-doubling material Yb:YAB[J]. *Journal of the Optical Society of America* B,2003,**20**(4):706-712.

[6] HU M H, NGUYEN H K, SONG K C, *et al*. High-power high-modulation-speed 1060-nm DBR lasers for green-light emission[J]. *IEEE Photonics Technology Letters*,2006,**18**(1-4):616-618.

[7] ACHTENHAGEN M. Transverse mode coupling in narrow-ridge waveguide laser diodes[J]. *Optics Communications*, 2006,**266**(1):172-174.

[8] PARK K H, LEE K, JANG D H, *et al*. Kink and beam steering free 0.98μm high-power RWG lasers with partially ion implanted channels[J]. *Electronics Letters*,1998,**34**(6):562-563.

[9] PAWLIK S, TRAUT S, THIES A, *et al*. Ultra-high power RWG laser diodes with lateral absorber region[C]. 2002 IEEE 18th International Semiconductor Laser Conference Conference Digest, 2002:163-164.

[10] SWINT R B, YEOH T S, ELARDE V C, *et al*. Curved waveguides for spatial mode filters in semiconductor lasers[J]. *IEEE Photonics Technology Letters*, 2004,**16**(1):12-14.

[11] WENZEL H, BUGGE F, DALLMER M, *et al*. Fundamental-lateral mode stabilized high-power ridge-waveguide lasers with a low beam divergence[J]. *IEEE Photonics Technology Letters*, 2008,**20**(3):214-216.

[12] TAN Shao-yang, ZHAI Teng, ZHANG Rui-kang, *et al*. Graded doping low internal loss 1060-nm InGaAs/AlGaAs quantum well semiconductor lasers[J]. *Chinese Physics B*, 2015,**24**(6):374-377.

[13] ZHAI Teng, TAN Shao-yang, LU Dan, *et al*. High power 1060 nm distributed feedback semiconductor laser[J]. *Chinese Physics Letters*, 2014,**31**(2):52-54.

[14] VAIL E C, NABIEV R F, CHANG-HASNAIN C J. Temperature dependence of light-current characteristics of 0.98-μm Al-free strained-quantum-well lasers[J]. *IEEE Photonics Technology Letters*, 1994,**6**(11):1303-1305.